

1 **Title: A circadian clock in the blood-brain barrier regulates xenobiotic efflux from the**
2 **brain**

3
4 **Authors:** Shirley L. Zhang^{1,2}, Zhifeng Yue^{2,3}, Denice M. Arnold², and Amita Sehgal^{2,3*}

5 **Affiliations:**

6 ¹Center for Sleep and Circadian Neurobiology, Perelman School of Medicine at the University of Pennsylvania.

7 ²Penn Chronobiology, Perelman School of Medicine at the University of Pennsylvania

8 ³Howard Hughes Medical Institute, Perelman School of Medicine at the University of Pennsylvania

9 *Correspondence to/lead contact: amita@mail.med.upenn.edu

10

11 **Highlights:**

- 12 • The *Drosophila* BBB displays a circadian rhythm of permeability
- 13 • Cyclic efflux driven by a clock in the BBB underlies the permeability rhythm
- 14 • Circadian control is non-cell-autonomous via gap junction regulation of $[Mg^{2+}]_i$
- 15 • An anti-seizure drug is more effective when administered at night

16

17 **Summary:** Endogenous circadian rhythms are thought to modulate responses to external factors, but
18 mechanisms that confer time-of-day differences in organismal responses to environmental insults/therapeutic
19 treatments are poorly understood. Using a xenobiotic, we find that permeability of the *Drosophila* “blood”-brain
20 barrier (BBB) is higher at night. The permeability rhythm is driven by circadian regulation of efflux and depends
21 upon a molecular clock in the perineurial glia of the BBB, although efflux transporters are restricted to
22 subperineurial glia (SPG). We show that transmission of circadian signals across the layers requires gap
23 junctions, which are expressed cyclically. Specifically, during nighttime gap junctions reduce intracellular
24 magnesium ($[Mg^{2+}]_i$), a positive regulator of efflux, in SPG. Consistent with lower nighttime efflux, nighttime
25 administration of the anti-epileptic phenytoin is more effective at treating a *Drosophila* seizure model. These
26 findings identify a novel mechanism of circadian regulation and have therapeutic implications for drugs targeted to
27 the central nervous system.

28

29 **Introduction:**

30 Circadian rhythms are endogenous, entrainable oscillations of biological processes that are dependent on a
31 molecular clock. The central clock that drives rhythmic behavior is located in the brain, but clocks are also found
32 in peripheral tissues where they exert local control over physiological functions (Ito and Tomioka, 2016; Mohawk
33 et al., 2012). Peripheral clocks share largely the same core clock machinery as the central clock, but target tissue-
34 specific genes, generating rhythms in many different physiological processes. Rhythms are observed in behaviors
35 such as sleep, secretion of many hormones, lipid and glucose metabolism as well as lung and cardiac function, to
36 mention just a few examples (Mohawk et al., 2012). Given the pervasive nature of circadian rhythms, it is
37 generally thought that the response of an organism to drugs/therapies must also vary with time of day (Dallmann
38 et al., 2016; Kaur et al., 2016). To date, the mechanisms suggested for such responses include rhythmic
39 expression of molecular targets and/or circadian rhythms in the responsiveness of the target tissue (Antoch et al.,
40 2005).

41

42 An additional obstacle for therapeutic drugs administered for the treatment of CNS disease is passage through
43 the blood brain barrier (Abbott, 2013). Higher concentrations of drug facilitate entry, but efficacy is limited by
44 dose-dependent toxicity of peripheral tissues; thus, many researchers have been engineering methods to improve
45 drug delivery to the CNS (Banks, 2016). The BBB in mammals consists of blood vessels surrounded by
46 endothelial tight junctions, which have many evolutionarily conserved adhesion and transport molecules (Ballabh
47 et al., 2004). Although *Drosophila* have a much more primitive circulatory system, they also have a barrier
48 between the hemolymph, insect “blood”, and the brain, composed of glial cells, which are structurally and
49 functionally similar to the mammalian BBB cells (DeSalvo et al., 2011, 2014). The similarity of BBB layers in
50 vertebrates and invertebrates strengthen the idea that BBB mechanisms are conserved, suggesting that novel
51 findings in invertebrate model organisms will have a significant impact on the understanding of vertebrate BBB
52 functions. The *Drosophila* BBB consists of a contiguous, flattened layer of subperineurial glia (SPG) and
53 perineurial glia (PG) that covers the entire central nervous system. The cells of the SPG have extensive contact
54 zones in which septate junctions prevent molecules from paracellular diffusion (Limmer et al., 2014). Transport of
55 molecules through the *Drosophila* BBB uses many of the same mechanisms as in the mammalian endothelial

56 BBB, including homologous membrane transport protein families such as the ATP-binding cassette (ABC)
57 transporter family, which includes p-glycoprotein (pgp) (DeSalvo et al., 2014; Mayer et al., 2009).

58

59 In this study, we examine xenobiotic permeability in *Drosophila* and find that it is dependent on a circadian clock
60 in the BBB. We find that the circadian clock-containing cells (PG) maintain oscillating gap junctions, which are
61 required to regulate the intracellular concentration of magnesium ions ($[Mg^{2+}]_i$) in the ABC-like transporter-
62 containing SPG cells. The rhythm in BBB permeability produces a rhythm of drug accumulation in the brain,
63 resulting in increased responsiveness of seizure-sensitive *Drosophila* to therapeutic drugs delivered at night.
64 These results reveal a novel mechanism of circadian regulation and suggest that therapeutic drugs targeting the
65 CNS should be given at optimal circadian times for BBB entry/retention to minimize the dosage and reduce toxic
66 side effects.

67

68 **Results**

69 **The blood-brain barrier contains a molecular clock that is required for a rhythm in xenobiotic retention**

70 To determine whether permeability of drugs to the brain varies with time of day, we first examined whether the
71 accumulation of rhodamine b (RHB), a xenobiotic, is different in iso31 (wild type) brains across the circadian day.
72 We injected female flies with RHB in the thorax and determined the amount of drug in the brain after 1 hr.
73 Although there was variability in the amount of RHB retained in the body across individual flies, the average
74 amount of dye in the body was similar between time points (Figure S1a). To account for the differences in
75 injections of individual flies, the amount of drug in the brain was normalized to the amount of drug remaining in the
76 rest of the body for each fly. RHB fluorescence in the brain showed a trough during midday and a peak in the
77 early night, demonstrating diurnal changes in permeability of the brain (Figure 1a). Using *period* null (*per*⁰) flies,
78 which are deficient in a core component of the molecular clock, we found that the diurnal oscillation in drug
79 retention was abolished (Figure 1b). To verify that the circadian cycle in permeability was not limited to RHB, we
80 assayed daunorubicin, another pgp substrate (Masuyama et al., 2012), and found a similar rhythm (Figure S1b).
81 These results show that permeability of the brain to xenobiotic drugs is dependent on the endogenous circadian
82 clock.

83

84 In *Drosophila*, as in mammals, core clock components are present in many tissues other than the central brain
85 clock neurons (Ito and Tomioka, 2016). We sought to determine whether the BBB has a functional molecular
86 clock by examining expression of the clock protein, PER, in the two groups of glia that constitute the *Drosophila*
87 BBB. Thus, we expressed GFP in the BBB using PG-specific (*NP6293-Gal4*) and SPG-specific (*moody-Gal4*)
88 drivers (Figure S1c) and looked for co-localization with PER. PER is undetectable in SPG cells (Figure S1d), but it
89 is expressed rhythmically in PG cells, such that daily changes in its levels and subcellular localization are
90 consistent with 24-hour oscillations of PER in the brain clock neurons (Figure 1c; Curtin et al., 1995; Ito and
91 Tomioka, 2016). These data identify a molecular clock within the PG cells of the BBB. To determine whether the
92 rhythm in permeability is dependent on the PG clock, we disrupted clock function specifically in PG cells. As the
93 tools for tissue-specific ablation of PER are not very effective, we used a dominant-negative version of the *per*
94 transcriptional activator, *cycle* (UAS-*dnCyc*) to disrupt the clock (Xu et al., 2008). Disrupting the circadian clock in
95 PG cells did not affect behavioral rhythms (Figure S1e), which are controlled by specific clock neurons in the brain
96 (Peschel and Helfrich-Förster, 2011). However, flies expressing UAS-*dnCyc* under the control of PG-Gal4 no
97 longer display nighttime increases of RHB retention in the brain compared to the genetic controls (Figure 2b),
98 suggesting that the PG clock is necessary for the circadian rhythm of permeability.

99

100 **Cyclic efflux, regulated non-cell-autonomously by the circadian clock, underlies the rhythm in BBB** 101 **permeability**

102 To determine the mechanisms that drive rhythms of permeability, we assessed RHB in *Drosophila* brains ex-vivo.
103 Brains were dissected, incubated in RHB, and immediately imaged with a confocal microscope following removal
104 of the RHB solution. The amount of RHB in the brains in the first frame was similar between dead flies and live
105 flies, showing that influx of RHB into the brain is via a passive mechanism (Figure S2a left panel). Further,
106 similarity in initial fluorescence between brains at zeitgeber time (ZT) 4-8 (ZT0=lights on and ZT12=lights off)
107 compared to ZT12-16 suggests negligible time-of-day differences in influx (Figure S2a right panel). Photo-
108 bleaching and passive diffusion from the brain were controlled using the loss in fluorescence of dead fly brains;
109 however, even after controlling for these factors, the level of drug in the live brains declined over an 8 minute
110 period. The loss of drug was greater in the brains during the daytime, ZT4-8, compared to early nighttime, ZT12-

111 16 (Figure 2a). Loss of drug was blunted when the p-glycoprotein (pgp) inhibitor verapamil was added, suggesting
112 that the reduction in RHB in the brain is due to active efflux by pgp-homologous transporters (Figure 2a). Higher
113 efflux during the day is consistent with lower permeability at this time, thereby providing a mechanism for the
114 rhythm in permeability.

115

116 Using an antibody that recognizes a highly conserved region of pgp, we stained for transporter expression at the
117 BBB and found colocalization with the SPG, but not the PG (Figure 2b). We then assessed the levels of pgp-like
118 transporter expression in the *Drosophila* brain at different times of day, but did not detect obvious oscillations in
119 either mRNA, measured by qPCR of pgp-like transporters Mdr65 and Mdr49, or protein, or observed by
120 immunofluorescence using the c219 anti-pgp antibody (Figure S2b-c). Together these results indicate that the PG
121 clock does not regulate expression of pgp-like transporters. We hypothesize that the PG clock regulates the
122 activity of pgp-like transporters present in the SPG.

123

124 **Cyclically-expressed gap junctions are required for the rhythm in BBB permeability**

125 To determine how pgp transporters are regulated by a non-cell autonomous clock, we considered mechanisms by
126 which SPG and PG cells might communicate with each other. As communication between barrier glia is thought
127 to be mediated by gap junctions (Speder and Brand, 2014; Weisburg et al., 1991), we assessed a possible role
128 for innexins. We first examined innexin expression in isolated BBB cells, using SPG-Gal4 and PG-Gal4 to drive
129 *mCD8GFP* and separating dissociated brains by fluorescence activated cell sorting (FACS); however, too few
130 cells were collected from even 100 brains for accurate mRNA measurements (Figure S3a). Fewer than 50 SPG
131 cells could be isolated per brain. Thus, we dissected whole brains to examine innexin mRNA levels and found that
132 *Inx1* (*ogre*) and *Inx2* both cycle in WT brains, but not in *per⁰* circadian clock mutants (Figure 3a).

133

134 We next determined whether blocking innexins prevents time-of-day signals from the PG from reaching the SPG.
135 Using an RNAi line previously reported to specifically knock down expression of *Inx1* which is enriched in glia
136 (Holcroft et al., 2013), we verified gene knock down by qPCR ((Speder and Brand, 2014); Figure S3b) and
137 expressed it in PG cells. Assays of permeability revealed loss of rhythm and an overall decrease in nighttime RHB
138 retention in PG-Gal4>UAS-*Inx1*^{RNAi} (*gd*) flies relative to Gal4 and UAS controls (Figure 3b). A second *Inx1*^{RNAi}

139 (TRiP) expressed in PG cells also exhibited arrhythmia in RHB permeability suggesting that the effect is not likely
140 due to genetic background (Figure S3c). Since *Drosophila* gap junctions rarely form homotypic channels (Phelan
141 and Starich, 2001), we examined whether inhibiting *Inx2* would also block oscillation of RHB permeability. As only
142 one RNAi line was available for *Inx2* and was lethal when expressed in all glial cells, we expressed a dominant-
143 negative form of *Inx2* (*UAS-dnInx2RFP*) (Speder and Brand, 2014) using the PG-Gal4 driver. Inhibition of *Inx2*
144 also resulted in loss of rhythmicity relative to controls (Figure 3c). Together these data suggest that gap junctions
145 *Inx1* and *Inx2* in PG cells are required for the oscillation of RHB efflux in the SPG. Thus, connectivity of the PG
146 and SPG via gap junctions appears to be important for relaying time-of-day signals. We further verified the
147 requirement for this connectivity by inhibiting gap junctions in the SPG, predicting that loss of gap junctions in the
148 SPG would also block intercellular communication. Indeed when we used SPG-Gal4 to drive *dnInx2*, we found a
149 similar loss of the RHB permeability rhythm (Figure 3d).

150

151 **Gap junctions drive cycling of intracellular magnesium concentrations in the SPG**

152 The requirement for gap junctions suggested involvement of a small second messenger that could diffuse through
153 these channels. Higher levels of $[Mg^{2+}]_i$ are known to increase *pgp* transporter activity (Booth et al.; Shapiros and
154 Ling, 1994), while increasing intracellular calcium ion concentration ($[Ca^{2+}]_i$) is thought to inhibit *pgp* activity (Liang
155 and Huang, 2000; Thews et al., 2006). We initially assessed $[Mg^{2+}]_i$ and $[Ca^{2+}]_i$ in both the PG and SPG using a
156 pan-BBB driver (9-137-Gal4). For $[Mg^{2+}]_i$ detection, we used the ratiometric fluorescent indicator *MagFura2* and
157 measured mean fluorescent intensity by flow cytometry (Figure S4a). We found that the $[Mg^{2+}]_i$ levels in the BBB,
158 labeled by 9-137-Gal4 driving *mCD8GFP*, cycle with a zenith at ZT2 and nadir at ZT14 (Figure S4b). For
159 measurements of $[Ca^{2+}]_i$, we used 9-137 to drive an NFAT-based sensor, *CaLexA* (calcium-dependent nuclear
160 import of Lex A) (Masuyama et al., 2012). This driver resulted in high specific expression of *CaLexA* with nearly
161 an absence of background noise in the *Drosophila* brain allowing for quantification of the fluorescence images
162 with a confocal microscope. We measured *CaLexA* signals across the circadian day and found an opposing
163 rhythm to $[Mg^{2+}]_i$ (Figure S4c). Importantly, the phase of these oscillations is consistent with high efflux transporter
164 activity during the day.

165

166 To address the dynamics of the ions in the subsets of the BBB, we labeled either the PG (PG-Gal4>UAS-
167 *mCD8RFP*) or the SPG (SPG-Gal4>UAS-*mCD8RFP*) and measured both magnesium and calcium in the same
168 brain sample, using Magfura2 along with the $[Ca^{2+}]_i$ indicator Cal630. In addition, we assessed the effect of
169 junctional communication on ionic concentrations. Thus, control brains or brains containing PG-Gal4>UAS-
170 *dnInx2RFP* or SPG-Gal4>UAS-*dnInx2RFP* were incubated with the ion indicators and analyzed by flow
171 cytometry. Interestingly, while control SPG had comparable levels of ions to the PG, inhibiting Inx2 function
172 resulted in higher $[Mg^{2+}]_i$ and lower $[Ca^{2+}]_i$ in the SPG compared to PG (Figure 4a). Because efflux transporters
173 regulated by magnesium/calcium ions are located in the SPG, we focused our efforts on this layer and found that
174 levels of $[Mg^{2+}]_i$ were cyclic, peaking early in the day and dropping at night (Fig 4b); however, no obvious cycle
175 was observed in $[Ca^{2+}]_i$ in the SPG (Figure S4d). Uncoupling the transporter-containing SPG from the clock-
176 containing PG using dnInx2 (SPG-Gal4>UAS-*dnInx2RFP*) abolished the cycling of $[Mg^{2+}]_i$ in the SPG (Fig 4c).
177 Together these data indicate that junctional communication equilibrates ionic concentrations across the two
178 layers; specifically, increased communication at night lowers magnesium in the SPG to reduce efflux transport
179 and promote permeability.

180

181 **Drug-mediated recovery from seizures is dependent on the BBB clock**

182 Since permeability of the BBB is dependent on the circadian clock, it seemed logical that the effect of xenobiotic
183 neuromodulatory drugs would also follow a rhythmic pattern based on how much drug is retained in the brain. To
184 test this idea, we fed an anti-seizure xenobiotic drug, phenytoin, to *easily-shocked* (*eas*) mutant flies, which are
185 sensitive to seizures induced by mechanical stimuli. Following 2 hrs of feeding on drug-containing media, the *eas*
186 mutants were vortexed and the number of flies paralyzed or seizing was recorded every 15 secs and the average
187 latency to recovery was calculated for each vial of flies at each time point. Overall, *eas* mutants receiving
188 phenytoin recover faster and so their latency to recovery is lower as compared to flies receiving vehicle (Figure
189 5a). We calculated the effect of the drug on recovery latency at different times of day, and found an increase in
190 drug efficacy at night (Figure 5b), which is consistent with the rhythm of BBB permeability we report here. While
191 there was some variability in the amount of phenytoin ingested by individual flies as measured by blue food dye
192 intake, there was no significant difference among time points (Figure S5). We infer that the increased efficacy of

193 the drug at night results from decreased pgp-mediated efflux, which increases nighttime retention and thereby
194 enhances neuromodulatory effects.

195

196 To determine whether the time-of-day-specific response of *eas* mutants to phenytoin was due to the circadian
197 clock in the BBB, we introduced the PG-Gal4 driver along with UAS *dnCyc* into the *eas* mutants. Unfortunately,
198 this genetic manipulation decreased the penetrance of the *eas* phenotype and therefore, altered the threshold of
199 seizure sensitivity so the magnitude of the drug-dependent change in recovery is not directly comparable to the
200 original *eas* mutants. Nonetheless, we assessed whether there were time-of-day differences in the response of
201 *eas* mutants to phenytoin in the absence of the PG clock (Figure 5c). Importantly, we found that there were no
202 circadian differences in drug response in the absence of the PG clock (Figure 5d). These results indicate the
203 clock in the BBB drives a rhythm in phenytoin-induced effects on the brain.

204

205 Discussion

206 We report here a rhythm of BBB permeability driven by a clock within the BBB, but through a novel, non-cell-
207 autonomous mechanism. These findings, which are the first to demonstrate a circadian rhythm in BBB
208 permeability, could account for previous findings of daily fluctuations in drug/hormone expression in the brain. For
209 instance, levels of leptin and cytokines were found to differ between the blood and the cerebrospinal fluid at
210 different times of day (Pan and Kastin, 2001; Pan et al., 2002). In addition, the level of quinidine, a pgp-effluxed
211 drug, in the rat brain depends on the timing of administration, with much lower levels of quinidine in the brain
212 during the animals' active period (Kervezee et al., 2014). We find that pgp function is regulated by the BBB clock
213 to efflux at a higher rate during the daytime, which is the active period of the fly, thus reducing the level of drug in
214 the brain. Similar regulation in the rat would account for the time-of-day changes in brain levels of quinidine.
215 Humans are diurnal, like flies, and so the human BBB would presumably display the same phase of efflux as that
216 observed in *Drosophila*.

217

218 Our results suggest that the molecular clock in the PG cells controls rhythms of *Inx1* and *Inx2*, which regulate
219 $[Mg^{2+}]_i$ levels within the SPG, thereby producing a cycle in the activity of the pgp transporters. Due to the high
220 levels of $[Mg^{2+}]_i$ in uncoupled SPG, we suggest that connectivity of the SPG to the PG via gap junctions acts as a

221 sink for $[Mg^{2+}]_i$, reducing the availability of $[Mg^{2+}]_i$ for transporter activity (Figure 6). Indeed, the initial rise in *Inx1*
222 and *Inx2* mRNA occurs in the early night, which coincides with the lowest levels of $[Mg^{2+}]_i$ within the SPG. The
223 finding that $[Mg^{2+}]_i$ couples circadian clocks to transporter activity in the *Drosophila* BBB provides an important
224 role for magnesium in circadian physiology in animals. Daily fluctuations in $[Mg^{2+}]_i$ also regulate cellular processes
225 in mammalian cell culture and single-celled algae (Feeney et al., 2016).

226

227 It is interesting that flies use non-cell autonomous mechanisms to drive a rhythm of BBB permeability, and fits
228 with the idea that clocks localize to specific cells in *Drosophila* and control behavior/physiology through circuits
229 (Chatterjee and Rouyer, 2016; Guo et al., 2014; Liang et al., 2017). However, given that one class of *Drosophila*
230 BBB cells contains clocks, these findings still raise the question of why clocks and transporters localize to different
231 cell types. We speculate that the two BBB layers have distinct functions that require different types of regulation
232 and activity. Indeed, BBB glia in *Drosophila* have recently been implicated in functions other than regulation of
233 the barrier, for instance in metabolic functions relevant for the brain (Volkenhoff et al., 2015). Given the generally
234 strong circadian influence in metabolic physiology, it is possible that the clock is located in PG cells to more
235 directly control metabolic activity, while the transporters need to be isolated from such processes.

236

237 While circadian studies have historically focused on neurons, glia have recently been gaining attention for their
238 contribution to the generation/maintenance of rhythms (Brancaccio et al., 2017; Damulewicz et al., 2013; Jackson
239 et al., 2015; Tso et al., 2017). However, the rhythms assayed in most of these cases are those of behavioral
240 locomotor activity and the relevant glia are usually astrocytes (Brancaccio et al., 2017; Jackson et al., 2015). The
241 role we report here for BBB glia indicates more general regulation of circadian physiology by glia. As noted
242 above, BBB glia are also implicated in metabolism, which might also be under circadian control.

243

244 (Xie et al., 2013) demonstrated that amyloid beta is cleared from the brain via a glymphatic system during sleep.
245 At first glance, these results may appear to contradict ours as they show increased clearance by the BBB during
246 sleep while we demonstrate higher efflux during the day; however, their model examined an endogenous protein
247 that is cleared largely by endocytic uptake followed by transcytosis (Yoon and Jo, 2012), rather than a xenobiotic
248 subject to *pgp*-mediated efflux. Also, Xie et al examined the differences as a function of behavioral state rather

249 than time-of-day. We suggest that these brain clearing systems are entirely compatible. Since animals encounter
250 xenobiotics primarily during their active period (i.e. through foraging, injury, etc), it would be evolutionarily
251 advantageous to be poised to immediately expel the foreign particle; however, endogenous proteins or
252 neurotoxins that slowly build up as a byproduct of brain functions during wakefulness may require a behavior shift
253 to sleep in order for them to be cleared. Future work may resolve whether the circadian regulation of the BBB
254 interacts with the sleep-dependent clearance of metabolites.

255

256 A major clinical implication of this work is the possibility of improving therapies with neuropsychiatric and
257 neurological drugs. Chronotherapy aligns medical treatments to the body's circadian rhythms, taking into
258 consideration circadian oscillations of the target tissue and rhythms in hormones, using the circadian information
259 to minimize side effects and optimize outcomes (Dallmann et al., 2014). A study of epileptic patients unresponsive
260 to standard doses of phenytoin and carbamazepine found that administration of all or most of the daily dose of
261 medication at night improved seizure control (Yegnanarayan et al., 2006). Our results suggest a model in which
262 the phase of BBB permissiveness is a key factor that determines therapeutic effects of xenobiotic drugs in the
263 brain. In support of regulated efflux as the basis of BBB permeability, higher levels of ppg in humans correspond
264 to a lack of responsiveness to seizure drugs (Loscher et al., 2011). Optimal timing of BBB transport and delivery
265 of drugs can be equally or more important as the timing of CNS responsiveness and should be considered in
266 administration of therapeutic regimens.

267

268 **References:**

- 269 Abbott, N.J. (2013). Blood-brain barrier structure and function and the challenges for CNS drug delivery. *J Inherit*
270 *Metab Dis* 36, 437–449.
- 271 Antoch, M.P., Kondratov, R. V, and Takahashi, J.S. (2005). Circadian clock genes as modulators of sensitivity to
272 genotoxic stress. *Cell Cycle* 4, 901–907.
- 273 Awasaki, T., Lai, S.L., Ito, K., and Lee, T. (2008). Organization and postembryonic development of glial cells in
274 the adult central brain of *Drosophila*. *J Neurosci* 28, 13742–13753.
- 275 Bainton, R.J., Tsai, L.T., Schwabe, T., DeSalvo, M., Gaul, U., and Heberlein, U. (2005). moody encodes two
276 GPCRs that regulate cocaine behaviors and blood-brain barrier permeability in *Drosophila*. *Cell* 123, 145–156.

277 Ballabh, P., Braun, A., and Nedergaard, M. (2004). The blood-brain barrier: an overview: structure, regulation,
278 and clinical implications. *Neurobiol Dis* 16, 1–13.

279 Banks, W.A. (2016). From blood-brain barrier to blood-brain interface: new opportunities for CNS drug delivery.
280 *Nat Rev Drug Discov* 15, 275–292.

281 Benzer, S. (1971). From the gene to behavior. *JAMA* 218, 1015–1022.

282 Booth, C.L., Pulaski, L., Gottesman, M.M., and Pastan, I. Analysis of the Properties of the N-Terminal Nucleotide-
283 Binding Domain of Human P-Glycoprotein.

284 Brancaccio, M., Patton, A.P., Chesham, J.E., Maywood, E.S., and Hastings, M.H. (2017). Astrocytes Control
285 Circadian Timekeeping in the Suprachiasmatic Nucleus via Glutamatergic Signaling. *Neuron* 93, 1420–1435.e5.

286 Chatterjee, A., and Rouyer, F. (2016). Control of Sleep-Wake Cycles in *Drosophila*.

287 Curtin, K.D., Huang, Z.J., and Rosbash, M. (1995). Temporally regulated nuclear entry of the *Drosophila* period
288 protein contributes to the circadian clock. *Neuron* 14, 365–372.

289 Dallmann, R., Brown, S.A., and Gachon, F. (2014). Chronopharmacology: new insights and therapeutic
290 implications. *Annu Rev Pharmacol Toxicol* 54, 339–361.

291 Dallmann, R., Okyar, A., and Levi, F. (2016). Dosing-Time Makes the Poison: Circadian Regulation and
292 Pharmacotherapy. *Trends Mol Med* 22, 430–445.

293 Damulewicz, M., Rosato, E., and Pyza, E. (2013). Circadian regulation of the Na⁺/K⁺-ATPase alpha subunit in
294 the visual system is mediated by the pacemaker and by retina photoreceptors in *Drosophila melanogaster*. *PLoS*
295 *One* 8, e73690.

296 DeSalvo, M.K., Mayer, N., Mayer, F., and Bainton, R.J. (2011). Physiologic and anatomic characterization of the
297 brain surface glia barrier of *Drosophila*. *Glia* 59, 1322–1340.

298 DeSalvo, M.K., Hindle, S.J., Rusan, Z.M., Orng, S., Eddison, M., Halliwill, K., and Bainton, R.J. (2014). The
299 *Drosophila* surface glia transcriptome: evolutionary conserved blood-brain barrier processes. *Front Neurosci* 8,
300 346.

301 Deshpande, S.A., Carvalho, G.B., Amador, A., Phillips, A.M., Hoxha, S., Lizotte, K.J., and Ja, W.W. (2014).
302 Quantifying *Drosophila* food intake: comparative analysis of current methodology. *Nat Methods* 11, 535–540.

303 Feeney, K.A., Hansen, L.L., Putker, M., Olivares-Yañez, C., Day, J., Eades, L.J., Larrondo, L.F., Hoyle, N.P.,
304 O'Neill, J.S., and van Ooijen, G. (2016). Daily magnesium fluxes regulate cellular timekeeping and energy

305 balance. *Nature* 532, 375–379.

306 Feng, Y., Ueda, A., and Wu, C.F. (2004). A modified minimal hemolymph-like solution, HL3.1, for physiological
307 recordings at the neuromuscular junctions of normal and mutant *Drosophila* larvae. *J Neurogenet* 18, 377–402.

308 Guo, F., Cerullo, I., Chen, X., and Rosbash, M. (2014). PDF neuron firing phase-shifts key circadian activity
309 neurons in *Drosophila*. *Elife* 3.

310 Holcroft, C.E., Jackson, W.D., Lin, W.H., Bassiri, K., Baines, R.A., and Phelan, P. (2013). Innexins *Ogre* and *Inx2*
311 are required in glial cells for normal postembryonic development of the *Drosophila* central nervous system. *J Cell*
312 *Sci* 126, 3823–3834.

313 Hughes, M.E., Hogenesch, J.B., and Kornacker, K. (2010). JTK_CYCLE: an efficient nonparametric algorithm for
314 detecting rhythmic components in genome-scale data sets. *J Biol Rhythm.* 25, 372–380.

315 Ito, C., and Tomioka, K. (2016). Heterogeneity of the Peripheral Circadian Systems in *Drosophila melanogaster*: A
316 Review. *Front Physiol* 7, 8.

317 Jackson, F.R., Ng, F.S., Sengupta, S., You, S., and Huang, Y. (2015). Glial cell regulation of rhythmic behavior.
318 *Methods Enzymol.* 552, 45–73.

319 Kaur, G., Phillips, C.L., Wong, K., McLachlan, A.J., and Saini, B. (2016). Timing of Administration: For Commonly-
320 Prescribed Medicines in Australia. *Pharmaceutics* 8.

321 Kervezee, L., Hartman, R., van den Berg, D.J., Shimizu, S., Emoto-Yamamoto, Y., Meijer, J.H., and de Lange,
322 E.C. (2014). Diurnal variation in P-glycoprotein-mediated transport and cerebrospinal fluid turnover in the brain.
323 *AAPS J* 16, 1029–1037.

324 Liang, X., and Huang, Y. (2000). Intracellular Free Calcium Concentration and Cisplatin Resistance in Human
325 Lung Adenocarcinoma A 549 Cells. *Biosci. Rep.* 20.

326 Liang, X., Holy, T.E., and Taghert, P.H. (2017). A Series of Suppressive Signals within the *Drosophila* Circadian
327 Neural Circuit Generates Sequential Daily Outputs. *Neuron* 94, 1173–1189.e4.

328 Limmer, S., Weiler, A., Volkenhoff, A., Babatz, F., and Klambt, C. (2014). The *Drosophila* blood-brain barrier:
329 development and function of a glial endothelium. *Front Neurosci* 8, 365.

330 Loscher, W., Luna-Tortos, C., Romermann, K., and Fedrowitz, M. (2011). Do ATP-binding cassette transporters
331 cause pharmacoresistance in epilepsy? Problems and approaches in determining which antiepileptic drugs are
332 affected. *Curr Pharm Des* 17, 2808–2828.

- 333 Masuyama, K., Zhang, Y., Rao, Y., and Wang, J.W. (2012). Mapping neural circuits with activity-dependent
334 nuclear import of a transcription factor. *J. Neurogenet.* 26, 89–102.
- 335 Mayer, F., Mayer, N., Chinn, L., Pinsonneault, R.L., Kroetz, D., and Bainton, R.J. (2009). Evolutionary
336 conservation of vertebrate blood-brain barrier chemoprotective mechanisms in *Drosophila*. *J Neurosci* 29, 3538–
337 3550.
- 338 Mohawk, J.A., Green, C.B., and Takahashi, J.S. (2012). Central and peripheral circadian clocks in mammals.
339 *Annu Rev Neurosci* 35, 445–462.
- 340 Pan, W., and Kastin, A.J. (2001). Diurnal variation of leptin entry from blood to brain involving partial saturation of
341 the transport system. *Life Sci* 68, 2705–2714.
- 342 Pan, W., Cornelissen, G., Halberg, F., and Kastin, A.J. (2002). Selected contribution: circadian rhythm of tumor
343 necrosis factor-alpha uptake into mouse spinal cord. *J Appl Physiol* 92, 1357–62; discussion 1356.
- 344 Peschel, N., and Helfrich-Förster, C. (2011). Setting the clock - by nature: Circadian rhythm in the fruitfly
345 *Drosophila melanogaster*. *FEBS Lett.* 585, 1435–1442.
- 346 Phelan, P., and Starich, T.A. (2001). Innexins get into the gap. *BioEssays* 23, 388–396.
- 347 Reynolds, E.R., Stauffer, E.A., Feeney, L., Rojahn, E., Jacobs, B., and McKeever, C. (2004). Treatment with the
348 antiepileptic drugs phenytoin and gabapentin ameliorates seizure and paralysis of *Drosophila* bang-sensitive
349 mutants. *J Neurobiol* 58, 503–513.
- 350 Shapiros, A.B., and Ling, V. (1994). THE JOURNAL OF BIOEGICAL CHEMISTRY ATPase Activity of Purified
351 and Reconstituted P-glycoprotein from Chinese Hamster Ovary Cells*. 269, 3745–3754.
- 352 Speder, P., and Brand, A.H. (2014). Gap junction proteins in the blood-brain barrier control nutrient-dependent
353 reactivation of *Drosophila* neural stem cells. *Dev Cell* 30, 309–321.
- 354 Stork, T., Engelen, D., Krudewig, A., Silies, M., Bainton, R.J., and Klambt, C. (2008). Organization and function of
355 the blood-brain barrier in *Drosophila*. *J Neurosci* 28, 587–597.
- 356 Thews, O., Gassner, B., Kelleher, D.K., Schwerdt, G., and Gekle, M. (2006). Impact of extracellular acidity on the
357 activity of P-glycoprotein and the cytotoxicity of chemotherapeutic drugs. *Neoplasia* 8, 143–152.
- 358 Tso, C.F., Simon, T., Greenlaw, A.C., Puri, T., Mieda, M., and Herzog, E.D. (2017). Astrocytes Regulate Daily
359 Rhythms in the Suprachiasmatic Nucleus and Behavior. *Curr. Biol.* 27, 1055–1061.
- 360 Volkenhoff, A., Weiler, A., Letzel, M., Stehling, M., Klambt, C., and Schirmeier, S. (2015). Glial Glycolysis Is

361 Essential for Neuronal Survival in *Drosophila*. *Cell Metab* 22, 437–447.

362 Weisburg, W.G., Barns, S.M., Pelletier, D.A., and Lane, D.J. (1991). 16S ribosomal DNA amplification for
363 phylogenetic study. *J. Bacteriol.* 173, 697–703.

364 Williams, J.A., Su, H.S., Bernard, A., Field, J., and Sehgal, A. (2001). A circadian output in *Drosophila* mediated
365 by neurofibromatosis-1 and Ras/MAPK. *Science* (80-.). 293, 2251–2256.

366 Xie, L., Kang, H., Xu, Q., Chen, M.J., Liao, Y., Thiyagarajan, M., O'Donnell, J., Christensen, D.J., Nicholson, C.,
367 Iliff, J.J., et al. (2013). Sleep drives metabolite clearance from the adult brain. *Science* (80-.). 342, 373–377.

368 Xu, K., Zheng, X., and Sehgal, A. (2008). Regulation of feeding and metabolism by neuronal and peripheral
369 clocks in *Drosophila*. *Cell Metab* 8, 289–300.

370 Yegnanarayan, R., Mahesh, S.D., and Sangle, S. (2006). Chronotherapeutic dose schedule of phenytoin and
371 carbamazepine in epileptic patients. *Chronobiol Int* 23, 1035–1046.

372 Yoon, S.-S., and Jo, S.A. (2012). Mechanisms of Amyloid- β Peptide Clearance: Potential Therapeutic Targets for
373 Alzheimer's Disease. *Biomol. Ther. (Seoul)*. 20, 245–255.

374 Zeng, H., Hardin, P.E., and Rosbash, M. (1994). Constitutive overexpression of the *Drosophila* period protein
375 inhibits period mRNA cycling. *EMBO J* 13, 3590–3598.

376

377

378 **Methods:**

379 **Fly stocks**

380 Iso31 flies are standard laboratory stocks. UAS-*dnCyc* was a gift from Dr. Paul Hardin (Zeng et al., 1994). *per*⁰
381 mutant flies and *eas*^{pc80} mutant flies were originally generated by Dr. Seymour Benzer (Benzer, 1971). The
382 following were obtained from the Bloomington Stock Center: UAS-*mCD8:GFP* (5137), UAS-*mCD8:RFP* (32218),
383 UAS-*nGFP* (4775), *repo-Gal4* (7415), *tubulin-GAL80^{ts}* (7016), UAS-*Inx1^{RNAi}* (TRiP, 27283). *Inx1^{RNAi}* (*gd*, 7136)
384 was from the Vienna *Drosophila* Resource Center. UAS-*dnInx2RFP* flies was a gift from Dr. Andrea Brand
385 (Speder and Brand, 2014). *NP6293-Gal4* was a gift from Dr. Mark Freeman (Awasaki et al., 2008). *moody-Gal4*
386 was a gift from Dr. Christian Klambt (Stork et al., 2008). *9-137-Gal4* (a P-element insertion line found in a screen
387 of a large P-GAL4 collection) was from Dr. Ulrike Heberlein, Janelia Farm Research Campus, VA. Gal4 lines were
388 outcrossed to Iso31 6x. UAS-*CaLexA* (*mLexA-VP16-NFAT*) flies were a gift from Dr. Jing Wang (Masuyama et
389 al., 2012).

390

391 **Permeability in fly brains**

392 5-7 day old adult female flies were entrained to 12:12 LD cycles. RHB and daunorubicin delivery methods are
393 similar to those previously described (Bainton et al., 2005). Briefly, a microinjection needle delivered intrahumoral
394 2.5 mg/mL RHB or 9 mg/ml daunorubicin in PBS between the posterior abdominal wall body segments of CO₂
395 anesthetized flies. Capillary action or positive pressure was applied to the needle under direct visualization over
396 1-2 secs to deliver an average volume of 50 nL per injection. Flies were given 1 hr after injection to rest and efflux
397 the RHB at 25°C. Brains from the flies were rapidly dissected in 1X PBS and washed with PBS before being
398 placed in 50 µL 0.1% SDS. Brains dissociated over >30 mins and the dye released from brain samples was
399 measured at excitation/emission: 540/590 using a Victor 3V (Perkin Elmer) plate reader. Bodies from the
400 corresponding flies were homogenized, spun down and measured at the same wavelengths. Uninjected flies were
401 used to adjust for background and the ratios of brain to body levels of RHB were calculated for individual flies or 5
402 flies were pooled for daunorubicin. Animals with less than 0.1 mg RHB injected into the body were excluded from
403 analysis due to increased variability of the brain:body ratio at brain RHB detection threshold. Amount of RHB was
404 calculated using a standard curve.

405

406 **Live imaging of fly brains RHB efflux**

407 Iso31 female flies were entrained to 12:12 LD cycles. Brains were carefully dissected in minimal hemolymph
408 solution HL3.1 (Feng et al., 2004) (70mM NaCl, 5mM KCl, 4 MgCl₂mM, 10mM NaHCO₃, 5mM trehalose, 115
409 sucrose, and 5mM HEPES, pH 7.4) with forceps with care to minimize damage to the surface of the brain. Brains
410 were incubated in 125 µg/mL RHB (Sigma, R6626) with or without verapamil (100 µg/mL) for 2 mins and washed
411 with HL3.1 media to image immediately. To determine the loss of fluorescence due to diffusion and
412 photobleaching during imaging, flies were microwaved for 1 min prior to brain dissection. Brains were imaged for
413 10 mins using a Leica SP5 confocal microscope. ImageJ software was used for analysis.

414

415 **Immunofluorescence**

416 Fly brains were dissected in cold PBS and fixed in 4% formaldehyde for 10 min on ice. Brains were rinsed 3 ×
417 10 min with PBS with 0.1% Triton-X (PBST), blocked for 30–60 min in 5% normal donkey serum in PBST (NDST),
418 and incubated overnight at 4°C in primary antibody diluted in NDST. Brains were then rinsed 4 × 10 min in PBST,
419 incubated 2 hrs in secondary antibody diluted in NDST, rinsed 4 × 10 min in PBST, and mounted with
420 Vectashield. Primary antibodies included anti-PGP C219 (10 µg/ml, ThermoFisher) and anti-PER UP1140
421 (1:1000, Cocalico Biologicals). Brains were imaged using a Leica SP5 confocal microscope. ImageJ software was
422 used for analysis.

423

424 **Rest:activity rhythms assays**

425 Locomotor activity assays were performed with the *Drosophila* Activity Monitoring System (Trikinetics) as
426 described previously (Williams et al., 2001). 5-7-day-old female flies were entrained to a 12:12 LD cycle for 3 days
427 then transferred to constant darkness for 5 days. Flies were maintained at 25°C throughout the assay.

428

429 **FACS sorting glial populations**

430 Brains were dissected in ice cold HL3.1 and were maintained on ice except during dissociation. Collagenase A
431 (Roche) and DNase I were added to final concentrations of 2 mg/mL and 20 units, respectively. Brains were
432 dissociated at 37°C using a shaker at 250 rpm for 20 mins pausing at 10 mins to pipette vigorously. Dissociated
433 tissue was filtered through 100 µm cell strainer and sorted using a 100 µm nozzle on a BD FACSAria (BD

434 Biosciences). Dead cells were excluded with 4,6-diamidino-2-phenylindole (DAPI). Doublets were excluded using
435 FSC-H by FSC-W and SSC-H by SSC-W parameters. GFP⁺ cells gates were set using according to GFP⁻ brain
436 tissue. Data were analyzed using FlowJo version 10.3 (Tree Star).

437

438 **Quantitative PCR**

439 Brains were dissected in cold PBS and immediately lysed. RNA was extracted using RNeasy mini kit (Qiagen)
440 and reverse transcribed to cDNA using random hexamers and Superscript II (Invitrogen). Real-time polymerase
441 chain reaction (PCR) was performed using Sybr Green PCR Master Mix (Applied Biosystems) with the
442 oligonucleotides described in Table 2. Assays were run on ViiA7 Real-Time PCR system (Applied Biosystems).
443 Relative gene expression was calculated using the $\Delta\Delta C_t$ method normalizing to actin.

444

Table S1.	Primers for real-time quantitative PCR	
Primer	Forward 5'→3'	Reverse 5'→3'
Actin	GGACCGGACTCGTCATACTC	CTGGCGGCACTACCATGTATC
Mdr65	CACGTCGTCCACCATGCTTT	TGCATCCGTGGTGATGTTCA
Mdr49	TCAGGGTGCAACCGGAGC	AGGCAAAGACCATTGACCGT

445

446 **Flow cytometric assay for intracellular magnesium and calcium levels**

447 Brains from entrained adult female flies (5-7 days) with fluorescently-labeled PG or SPG were dissected in adult
448 hemolymph-like saline (AHL; 108mM NaCl, 5mM KCl, 2mM CaCl₂, 8.2mM MgCl₂, 4mM NaHCO₃, 1mM NaH₂PO₄-
449 H₂O, 5mM trehalose, 10mM sucrose, 5mM HEPES; pH 7.5) on ice. Brains were brought to room temperature
450 (RT) for 10 mins and incubated with 5 μ M Magfura2-AM (ThermoFisher) and 5 μ M Cal630-AM (AAT Bioquest) for
451 20 mins at RT. Brains were washed with RT AHL for 3 x 5 mins. Then Collagenase A (Roche) and DNase I
452 (Sigma) were added to final concentrations of 2 mg/mL and 20 units, respectively and brains were dissociated at
453 37°C with 250 rpm shaking for 15 mins. Dissociated tissue was filtered through 100 μ m cell strainer and washed
454 with FACS buffer (PBS with 1% w/v bovine serum albumin and 0.1% w/v sodium azide). Cells were analyzed on
455 BD FACSCanto II (BD Biosciences). Doublets were excluded using FSC-H by FSC-W and SSC-H by SSC-W
456 parameters. RFP⁺ cells gates were set according to RFP⁻ brain tissue. Data were analyzed using FlowJo version
457 10.3 (Tree Star).

458

459 **Seizure recovery assay**

460 7-14 day old adult female *eas*^{PC80} flies were starved for 24 hrs to allow for maximum drug dosing. Flies were given
461 5% sucrose and 1.5% agar with or without 0.6 mg/mL phenytoin (Sigma), a previously described dose to improve
462 recovery from seizure (Reynolds et al., 2004). Flies were tested in 2 vials (1 control and 1 phenytoin), each
463 containing 15 flies. Mechanical shock was delivered by vortexing flies at high speed for 5 secs. The assays were
464 video recorded and the number of flies seizing was recorded at 15 sec intervals until the entire population had
465 recovered. Recovery was defined as standing and was analyzed by a researcher blinded to the drug condition.
466 Mean recovery time was calculated as the average time it took any individual fly to recover in a population. Flies
467 that never seized were calculated as 0 secs for recovery time.

468

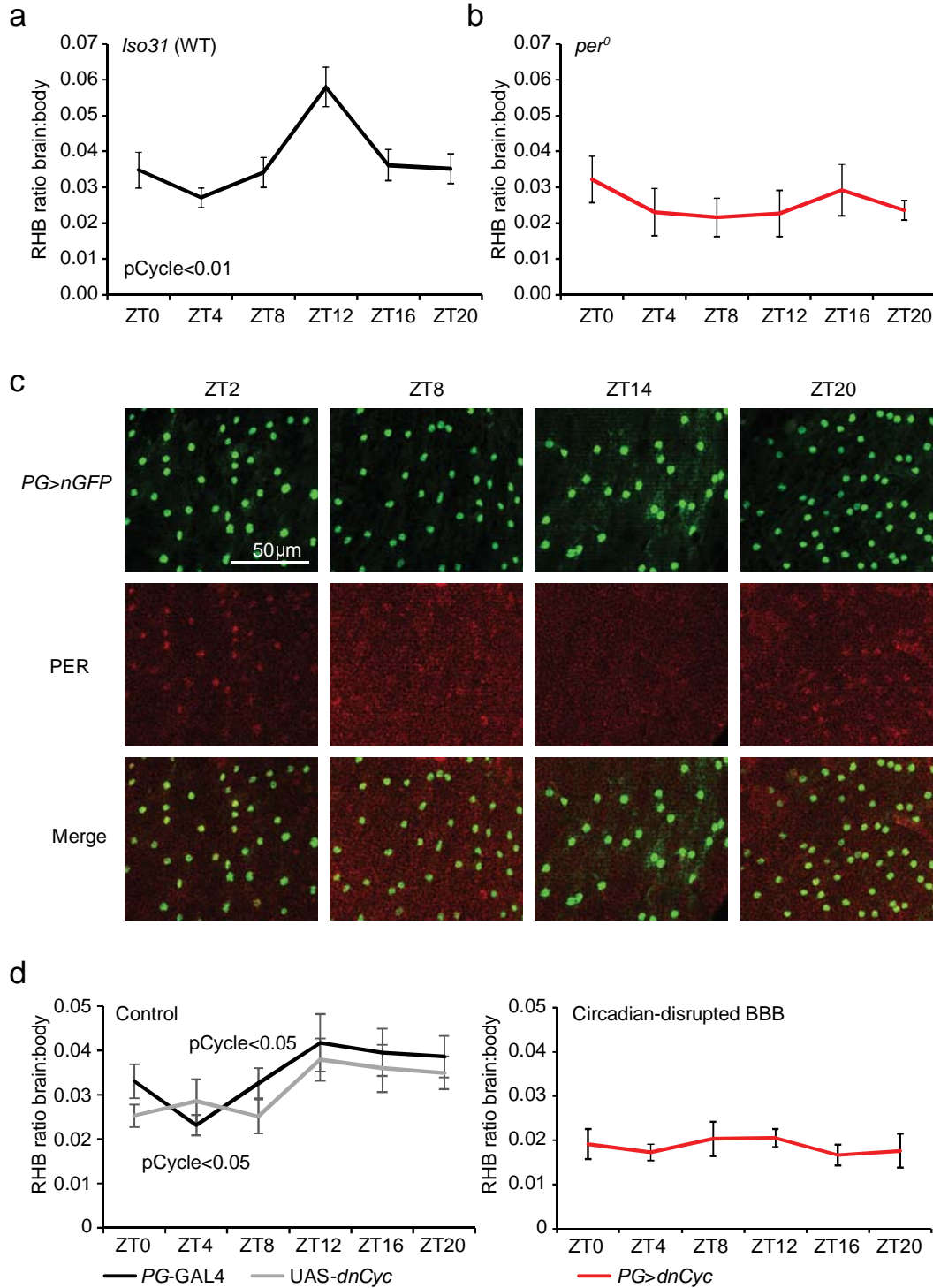
469 The blue dye feeding assay was performed as previously described (Deshpande et al., 2014). Briefly, after 24 hrs
470 of starvation, flies were given food with 2% w/v FD&C Blue No. 1 for 2 hrs. Individual flies were homogenized and
471 the absorbance at 620 nm was measured with a Victor 3V (Perkin Elmer) plate reader. The amount of food eaten
472 was calculated by using a standard curve.

473

474 **Statistical Analysis**

475 Circadian statistical analysis was performed in R using JTK_CYCLEv3.1(Hughes et al., 2010). ANOVA and post-
476 hoc Tukey tests were performed with Prism (GraphPad). Sample sizes were determined with
477 powerandsamplesize.com.

478



479

480 **Figure 1. A circadian clock in the *Drosophila* BBB regulates RHB permeability of the brain. (a and b)**

481 Rhythm of permeability into the *Drosophila* brain: Flies were injected with RHB under CO₂ anesthesia at different
482 time points and the levels of RHB in individual fly brains and bodies were measured after 1 hr using a
483 fluorescence reader at Ex540/Em595. The level of RHB fluorescence in the brain was normalized to the amount

484 of RHB in the body to control for injection consistency. Shown are the brain:body ratios of RHB in a) iso31 n=14-
485 21 per time point, pooled from 3+ experiments and b) *per^ρ* flies. n=8-21, pooled from 2 experiments. Means ±
486 SEM are shown. c) Expression of the PER clock protein in the BBB. PG-Gal4>UAS-*nGFP* *Drosophila* were
487 entrained to a 12:12 LD cycle for 3 days. The brain was analyzed for *nGFP* and PER expression at ZT2, ZT8,
488 ZT14, and ZT20 with a confocal microscope. Representative images of the surface of the brain are shown. Each
489 panel represents an area 100x120µm. d) The BBB clock is required for the permeability rhythm. PG-Gal4
490 (control), UAS-*dnCyc* (control), and PG-Gal4>UAS-*dnCyc* (experimental) were injected with RHB under CO₂
491 anesthesia and assessed by Ex540/Em595 fluorescence after 60 mins. Means ± SEM of the ratio of brain:body
492 fluorescence are depicted. n=12-22, pooled from 3 experiments. pCycle indicates a presence of rhythm using JTK
493 cycle analysis.

494

495 **Figure 2. Pgp-homologous**
496 **transporters in the SPG**
497 **regulate diurnal differences**

498 **in efflux of RHB.** a) Efflux
499 from the *Drosophila* brain. Live
500 brains from WT Iso31 flies at

501 ZT4-8 or ZT12-16 were
502 dissected in HL3.1 media and

503 incubated with RHB with or
504 without verapamil for 2 mins.

505 Dye was washed off and were
506 immediately imaged with a

507 confocal microscope.
508 Representative images are

509 shown (top panel). Adjusted
510 change in fluorescence of live

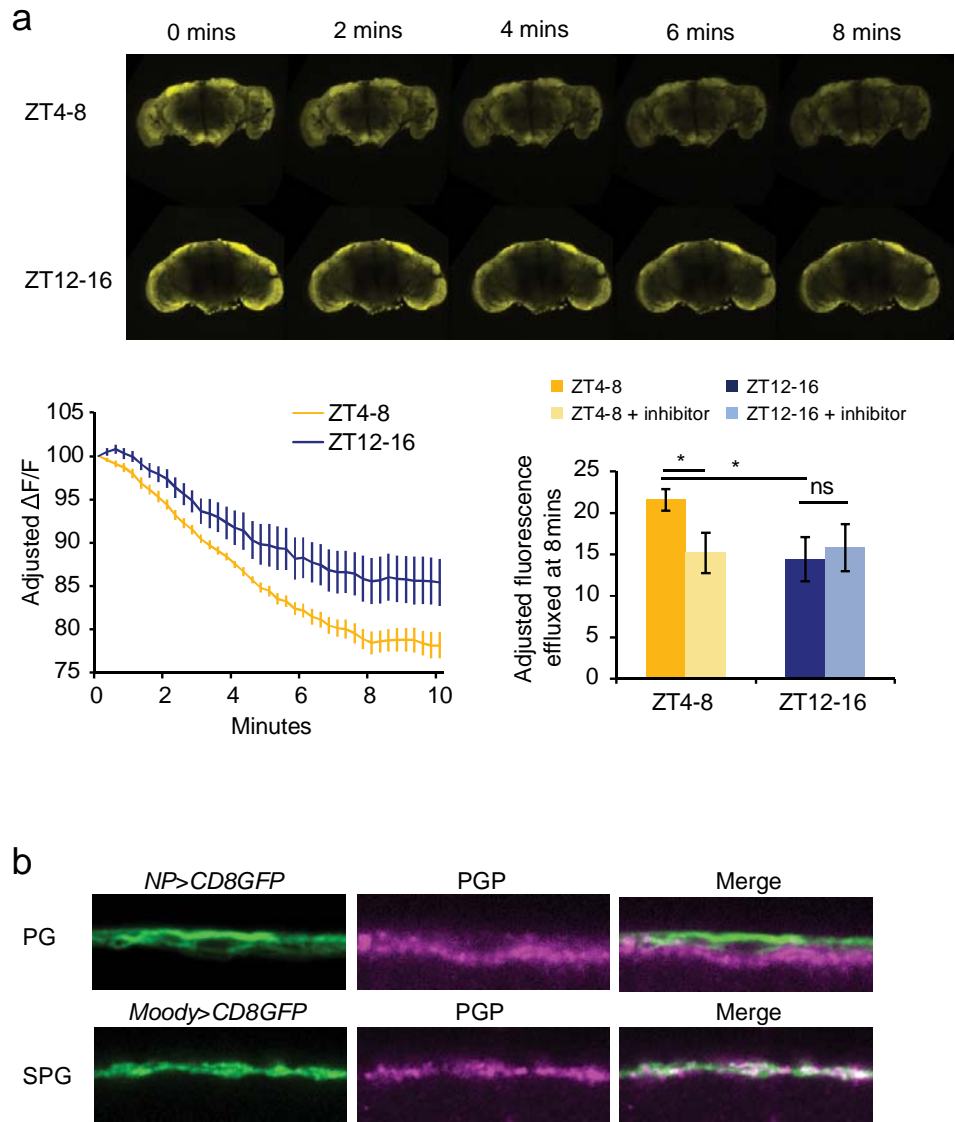
511 brains over time between
512 brains imaged at ZT4-8

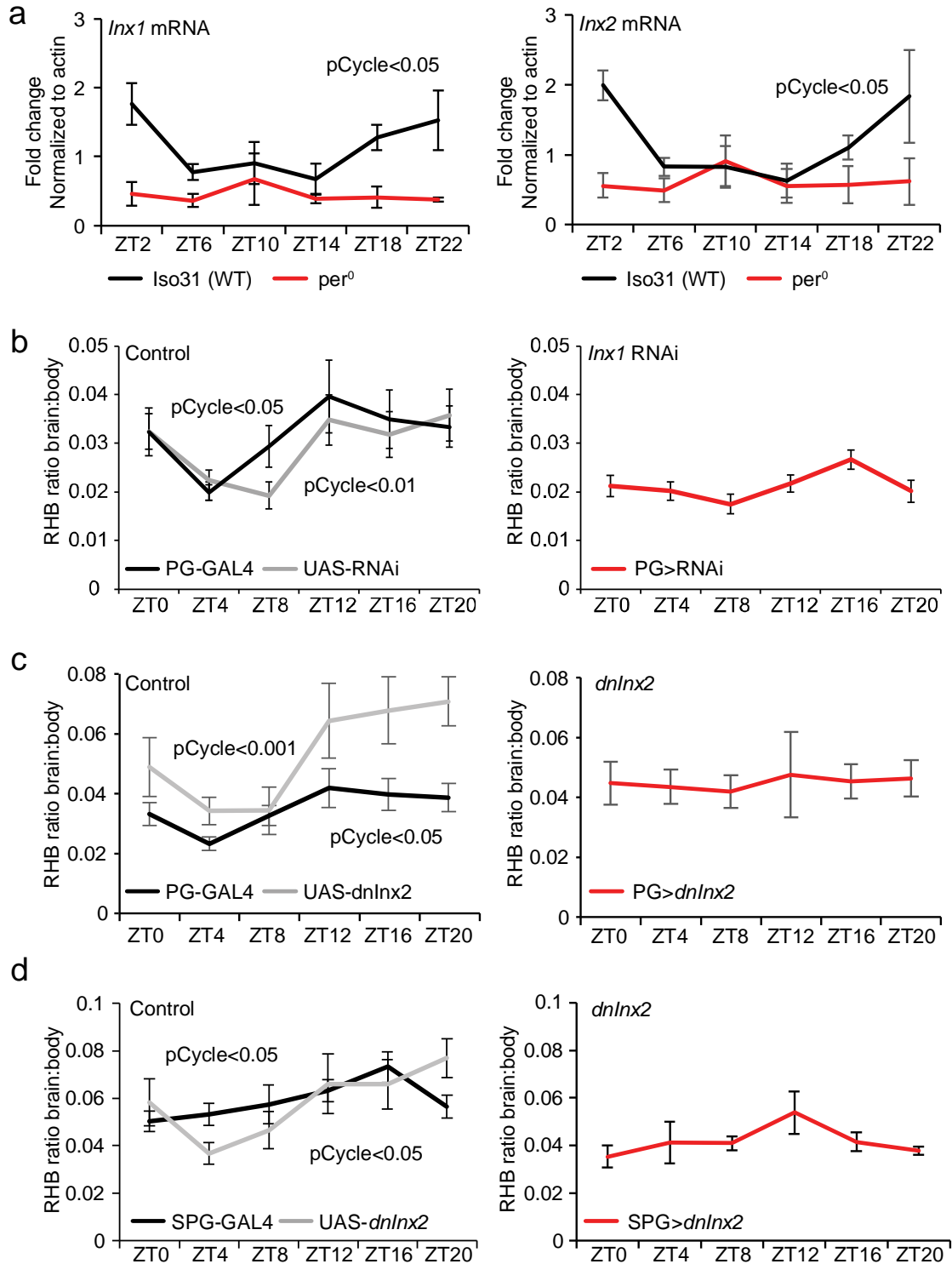
513 compared with ZT12-16 was
514 quantified (bottom left panel) and the time points incubated with verapamil compared at 8 mins (bottom right panel). n=7-8 brains, pooled from 2 independent experiments.

515 b) Expression of p-glycoprotein in the BBB. Brains
516 from PG-Gal4>UAS-*mCD8GFP* (top panels) or SPG-Gal4>UAS-*mCD8GFP* (bottom panels) were dissected and

517 incubated with c219 anti-pgp antibody and imaged with a confocal microscope. Pgp expression co-localized with
518 the SPG, but not the PG. Representative images of GFP expression (left), ppg fluorescence (center), and overlay
519 (right) are shown.

520



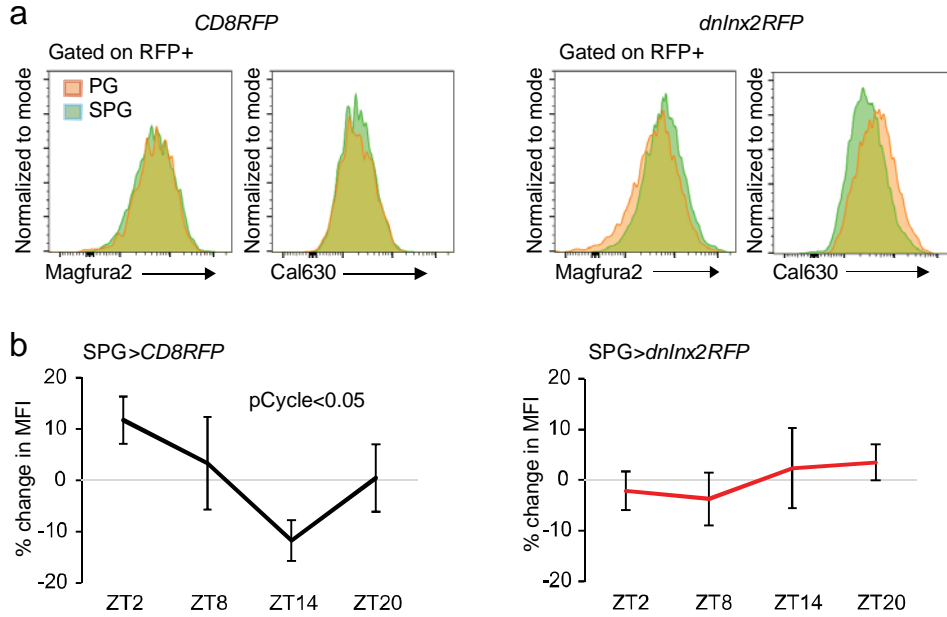


521

522 **Figure 3. Circadian signals from the PG to the SPG require gap junctions.** a) Expression of *Inx1* and *Inx2*
 523 across the day. Brains from WT and *per*⁰ flies were dissected and mRNA levels of *Inx1* (left panel) and *Inx2* (right
 524 panel) were measured by qPCR. (b-d) Effects of inhibiting gap junctions on the permeability rhythm. PG-

525 Gal4>UAS-*Inx1*^{RNAi} (gd) (b) or PG-Gal4>UAS-*dnInx2* (c) and corresponding genetic control flies were injected
526 with RHB at different time points and the levels of RHB in individual fly brains and bodies were assessed by
527 Ex540/Em595 fluorescence after 1 hr. Means \pm SEM of the ratio of brain:body are shown. n=10-22, pooled from
528 2+ experiments. pCycle indicates a presence of rhythm using JTK cycle analysis. SPG-Gal4>UAS-*dnInx2* (d) and
529 corresponding genetic control flies were injected with RHB at different time points and the levels of RHB in
530 individual fly brains and bodies were assessed by Ex540/Em595 fluorescence after 1 hr. Means \pm SEM of the
531 ratio of brain:body are shown. n=9-17, pooled from 3 experiments. pCycle indicates a presence of rhythm using
532 JTK cycle analysis.

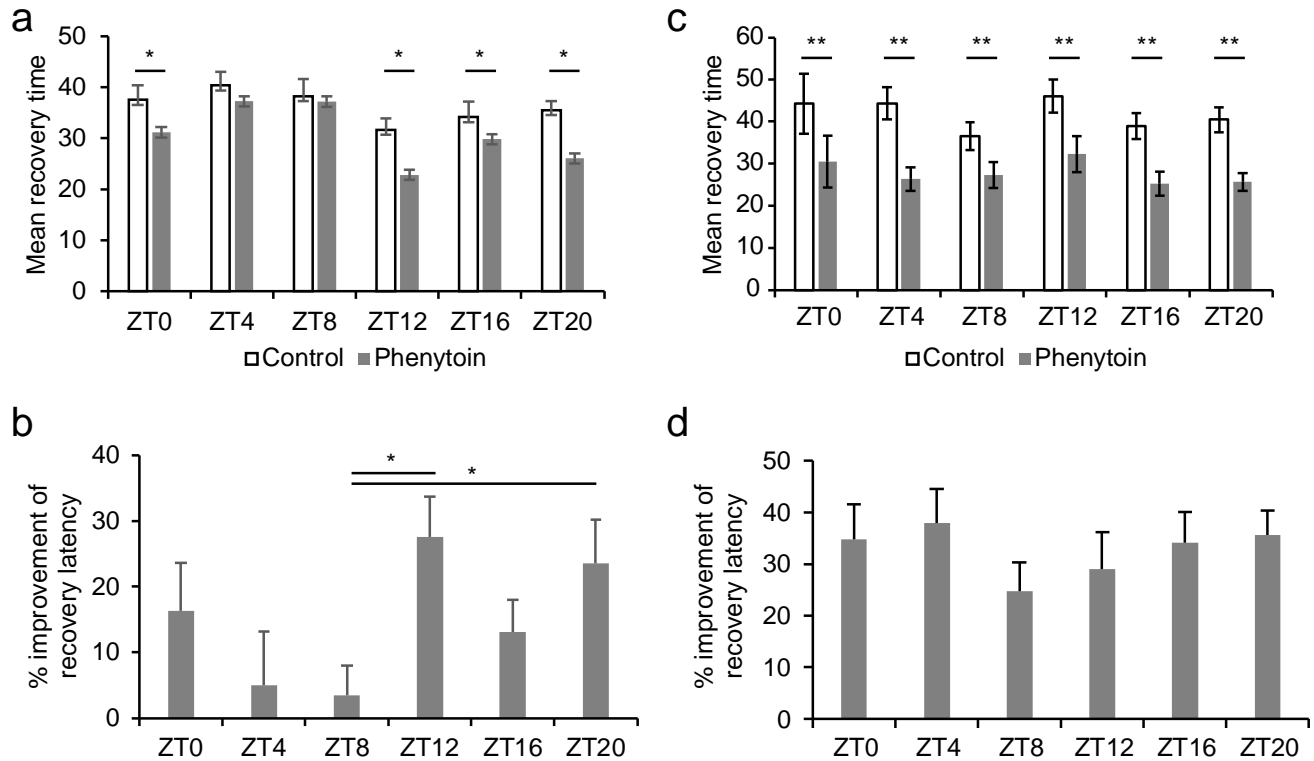
533



534

535 **Figure 4. Functional gap junctions are necessary for $[Mg^{2+}]_i$ cycling in the SPG.** a) Expression of
536 magnesium and calcium in BBB layers. Dissected brains from PG-Gal4>UAS-*mCD8RFP*, SPG-Gal4>UAS-
537 *mCD8RFP*, PG-Gal4>UAS-*dnInx2RFP*, or SPG-Gal4>UAS *dnInx2RFP* were incubated with $[Mg^{2+}]_i$ indicator and
538 $[Ca^{2+}]_i$ indicator, dissociated, and analyzed by flow cytometry. n=3 from 3 independent experiments.
539 Representative plots are shown. b) Effects of blocking gap junctions on magnesium rhythms in the SPG. SPG-
540 Gal4>UAS-*mCD8RFP* or SPG-Gal4>UAS-*dnInx2RFP* from brains at ZT2, ZT8, ZT14, ZT20 were incubated with
541 $[Mg^{2+}]_i$ indicator dissociated, and analyzed by flow cytometry. The percent changes in mean fluorescent intensity
542 (MFI) of the indicator is shown as means \pm SEM. n=4 from 3 experiments. pCycle indicates a presence of rhythm
543 using JTK cycle analysis.

544

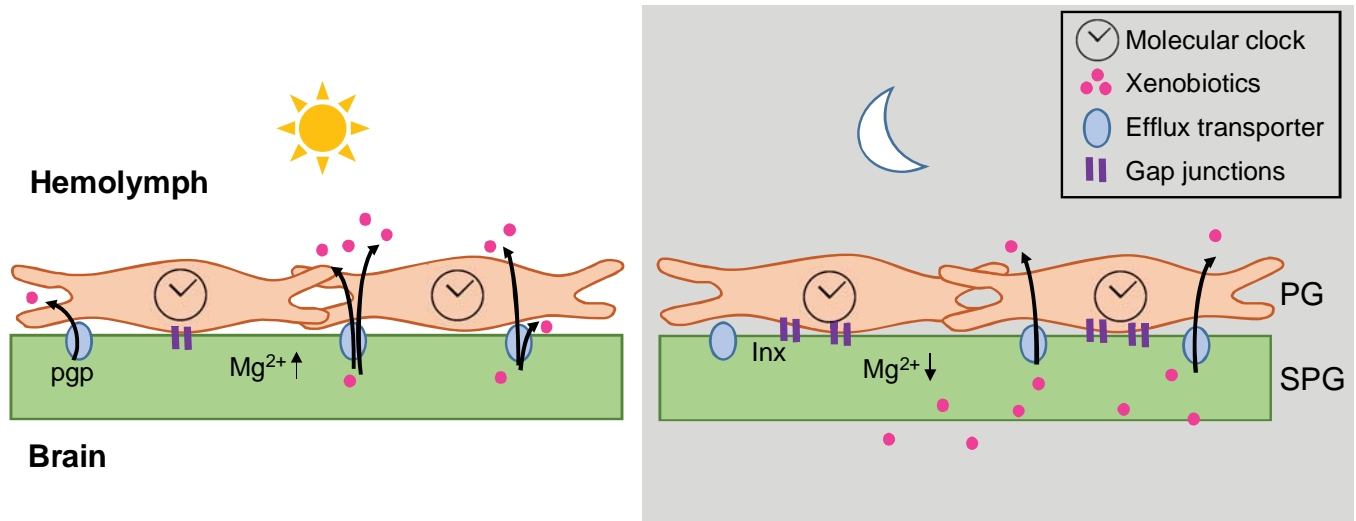


545

546 **Figure 5. Effect of phenytoin on seizure mutants is dependent on the clock.** 15-20 *eas* mutants were
 547 entrained to a 12:12 LD cycle for >3 days, starved for 24 hrs, and fed vehicle or phenytoin for 2 hrs in agar vials.
 548 Seizures were induced by mechanical stimulation and the number of seizing flies was counted every 15 secs to
 549 calculate mean recovery for each vial. a) Means \pm SEM of average recovery latency for each vial, * p <0.05
 550 between vehicle-treated vials and phenytoin-treated vials are shown by paired Student's t-test. b) Means + SEM
 551 of the percentage difference in recovery latency between vehicle and phenytoin are shown. Statistical analysis
 552 was performed with one-way ANOVA with post-hoc multiple comparisons Tukey test * p <0.05. c) 15 *eas* mutants
 553 with *NP6293-Gal4>UAS-dnCyc* were entrained and fed vehicle or phenytoin as described above. Means \pm SEM
 554 are shown. ** p <0.01 between vehicle-treated vials and phenytoin-treated vials are shown by Student's t-test. d)
 555 Means + SEM of the percentage difference in the recovery latency between vehicle and phenytoin. Unfortunately
 556 we are unable to directly compare recovery times of *eas* mutants with *eas* mutants carrying *PG-Gal4>UAS-dnCyc*
 557 due to the differences in seizures and kinetics of recovery. All time points of the *eas* mutants with *PG-Gal4>UAS-*
 558 *dnCyc* had greater recovery latency but fewer seizing flies at baseline without drug.

559

560



561
562

Figure 6. Model of circadian regulation of BBB efflux. During the day, circadian clock regulation in the PG lowers levels of gap junctions, reducing connectivity with the SPG. The level of $[Mg^{2+}]_i$ is high in the SPG, which promotes activity of the efflux transporters, reducing permeability of xenobiotics. During the night, the PG clock increases gap junctions, thereby increasing connectivity with the SPG. The Mg^{2+} ions diffuse from SPG into the PG, lowering the $[Mg^{2+}]_i$ in the SPG. The efflux transporters have reduced activity due to the decline in $[Mg^{2+}]_i$ and xenobiotics are retained in the brain.

568

Acknowledgments: This work was supported by grants T32HL07713 and R25MH060490 from the National Institutes of Health (S.L.Z.) and the Howard Hughes Medical Institute (A.S.). S.L.Z. and A.S. designed the experiments. S.L.Z., Z.Y., and performed the research. S.L.Z., Z.Y., D.M.A, and A.S. collected, analyzed, and interpreted the data. S.L.Z., and A.S. wrote and edited the paper. We thank Dr. John Hogenesch for assistance with statistical analysis. The authors have no financial conflicts to disclose.

574

575